

NUMERICAL ANALYSIS PROJECT  
MANUSCRIPT NA-92-15

OCTOBER 1992

**Fast Solution of the Helmholtz Equation  
with Radiation Condition by Imbedding**

by

Oliver Ernst

NUMERICAL ANALYSIS PROJECT  
COMPUTER SCIENCE DEPARTMENT  
STANFORD UNIVERSITY  
STANFORD, CALIFORNIA 94305





# FAST SOLUTION OF THE HELMHOLTZ EQUATION WITH RADIATION CONDITION BY IMBEDDING

OLIVER ERNST

October 2, 1992

## 1. INTRODUCTION

The exterior scattering problem is a common problem in **electromagnetics** and acoustics and consists in finding the field generated by a body on which a wave is impinging. If the **occurring** wave is assumed to have harmonic time dependence and constant propagation speed, the field is given by the solution of the Helmholtz or reduced wave equation

$$-\Delta u - k^2 u = f,$$

where the wave number  $k$  is a real constant. If we denote the (assumed smooth) boundary of the scattering body by  $\gamma$  and the region exterior to it by  $\mathcal{D}$ , the problem to be solved is

$$\begin{aligned} (1) \quad & -\Delta u - k^2 u = f \text{ in } \mathcal{D}, \\ (2) \quad & u = g \text{ on } \gamma \\ (3) \quad & \lim_{r \rightarrow \infty} r^{\frac{d-1}{2}} (u_r - iku) = 0. \end{aligned}$$

Here,  $d$  is the dimension of the underlying space,  $f$  and  $g$  are given functions and (3) is the Sommerfeld radiation condition. The latter can be interpreted as a boundary condition imposed at infinity; it serves to specify a unique solution, in this case consisting of only outgoing waves. Rather than the Dirichlet boundary condition (2), Neumann, impedance or mixed linear boundary conditions could also be considered.

In this paper, we introduce a very efficient method for solving this problem numerically. It employs a finite difference discretization using a regular grid on a bounded computational domain  $\Omega \subset \mathcal{D}$ . The resulting linear system of equations is solved by a fast Poisson solver. The incorporation of the radiation condition results in the addition of only very few steps of an iterative method for solving linear systems to the overall solution algorithm if a cyclic reduction based fast solver is used, and no iteration at all is necessary for a fast solver based on Fourier techniques. Finally, the inclusion of the possibly irregularly shaped boundary  $\gamma$  of the scatterer into the regular grid necessary for the fast solver is accomplished with an imbedding technique known as the capacitance matrix method.

---

**This work was supported by the National Science Foundation under Grant NSF CCR-8821078.**

When attempting to solve this problem with discretization methods, the infinite domain must be truncated to a so-called *computational domain*, which we shall denote by  $\Omega$ , on which an approximate solution is sought. This introduces an artificial boundary, denoted by  $\mathcal{B}$ , so that  $\partial\Omega = \gamma \cup \mathcal{B}$ . In reformulating the problem on the domain  $\Omega$ , the question arises as to how to translate the Sommerfeld condition to a boundary condition on  $\mathcal{B}$  to yield a well-posed problem. Ideally, the boundary condition should result in a problem the solution of which is the restriction to  $\Omega$  of the solution of (1)-(3). Boundary conditions having this property are known as *exact boundary conditions*. A great advantage of exact boundary conditions is that they allow the artificial boundary to be placed very close to the scatterer, thus reducing the computational effort. This contrasts with a class of approximations to (3) which are valid in an asymptotic sense, i.e. yield better approximations the further away the artificial boundary is placed from the body, cf. [1]. Finally, the boundary condition on  $\mathcal{B}$  should be easily incorporated into the numerical method being used to solve the problem on  $\Omega$ .

We have chosen to use the boundary condition devised by Keller and Givoli in [9], which is applicable if the artificial boundary  $\mathcal{B}$  is a circle or a sphere. It is an exact boundary condition which specifies the normal derivative  $u_n$  of the solution  $u$  on  $\mathcal{B}$  as an expression involving a surface integral of  $u$  over  $\mathcal{B}$ . The mapping thus defined is called the *Dirichlet to Neumann (DtN) map*, since it relates Dirichlet data to Neumann data on the artificial boundary. Even though this is not a local boundary condition in the sense that the prescribed values of  $u_n$  depend on the values of  $u$  on all of  $\mathcal{B}$ , it can be very efficiently integrated into the finite difference scheme, as will be shown below.

The paper is organized as follows. In section 2, we describe the finite difference discretization of the Helmholtz equation on an **annulus** and the resulting linear system of equations as well as the two orderings of the unknowns which permit two classical fast solvers to be used for its solution. Section 3 gives a derivation of the **DtN** mapping used to specify the exact radiation boundary condition and shows how it is incorporated into the discrete problem. The imbedding of the scatterer into the problem on the regular grid is described in section 4 and numerical results are collected in section 5.

**1.1. Acknowledgment.** The author would like to thank his advisor G.H. Golub for continuing support and guidance as well as J.B. Keller for introducing him to the **DtN** boundary condition.

## 2. FAST SOLVERS

Since all but the most crude approximations of the Sommerfeld condition at infinity include expressions involving the distance to some origin, the problem is most naturally formulated in polar coordinates  $(x, y) = (r \cos \theta, r \sin \theta)$ . In this coordinate system, the Helmholtz operator as well as most local approximations to the Sommerfeld condition still allow for the separation of variables, so that classical fast solvers can be used to solve the discrete problem. One such algorithm is described in [13] and the derivation in this section largely follows that there. Since the fast solver will be used in conjunction with an imbedding method which centers the scatterer at the origin, it suffices to provide a fast solver on an **annulus**  $\mathcal{A}(\rho_0, \rho_1) = \{(x, y) \in \mathbb{R}^2 \mid \rho_0^2 < x^2 + y^2 < \rho_1^2\}$  with a Dirichlet boundary condition

imposed on the inner boundary  $r = \rho_0$  and a Neumann boundary condition on the outer boundary  $r = \rho_1$ . The inner radius  $\rho_0$  will then be chosen small enough for the corresponding circle to lie completely within the imbedded body. This also avoids the coordinate singularity at the origin/

In polar coordinates, the Helmholtz equation takes on the form

$$(4) \quad \frac{1}{r}(ru_r)_r - \frac{1}{r^2}u_{\theta\theta} - k^2u = f.$$

To discretize the radial and angular coordinates, we now choose two positive integers  $m$  and  $n$  and define the grid spacings to be  $\Delta r = (\rho_1 - \rho_0)/m$  and  $\Delta\theta = 2\pi/n$ . The grid then consists of the points  $(r_i, \theta_j)$  where

$$\begin{aligned} r_i &= \rho_0 + i\Delta r & i &= 0, 1, \dots, m \\ \theta_j &= j\Delta\theta & j &= 1, \dots, n. \end{aligned}$$

To find approximations  $u_{i,j}$  to the values  $u(r_i, \theta_j)$  of the solution at the grid points, we perform the usual Taylor series expansion of  $u$  about a grid point to arrive at the following finite difference formula with a truncation error of  $O(\Delta r^2 + \Delta\theta^2)$ :

$$(5) \quad \begin{aligned} & \frac{1}{r_i\Delta r^2} [r_{i+1/2}(u_{i+1,j} - u_{i,j}) - r_{i-1/2}(u_{i,j} - u_{i-1,j})] \\ & - \frac{1}{r_i^2\Delta\theta^2} [u_{i,j+1} - 2u_{i,j} + u_{i,j-1}] - k^2u_{i,j} = f_{i,j}. \end{aligned}$$

To apply the Dirichlet boundary condition at  $r = \rho_0$ , we replace  $u_{0,j}$  with  $g(\theta_j)$  in the equations corresponding to the grid points  $(r_1, \theta_j)$ . The Neumann condition

$$u_r(\rho_1, \theta) = h(\theta)$$

is approximated by

$$\frac{u_{m+1,j} - u_{m-1,j}}{2\Delta r} = h(\theta_j),$$

where the fictitious values  $u_{m+1,j}$  are eliminated by inserting

$$u_{m+1,j} = u_{m-1,j} + 2\Delta r h(\theta_j)$$

into the equation (5) corresponding to the grid points  $(r_m, \theta_j)$ .

**2.1. An ordering permitting cyclic reduction.** We order the unknowns by grouping together those on the same ray, moving outward on each ray. This results in a linear system of equations

$$\tilde{B}\mathbf{u} = \mathbf{f},$$

the matrix of which has the block structure

$$\tilde{B} = \begin{bmatrix} A + 2D & -D & & & -D \\ -D & A + 2D & -D & & \\ & & \ddots & \ddots & \ddots \\ & & & -D & A + 2D & -D \\ -D & & & & -D & A + 2D \end{bmatrix},$$



Systems with this structure can be solved using the well-known cyclic reduction algorithm in  $O(mn \log n)$  arithmetic operations, cf. [3] or [14].

**2.2. An ordering suitable for Fourier techniques.** Ordering instead along the concentric circles of grid lines, the scaled coefficient matrix is given by the Kronecker sum

$$B_F := I_m \otimes T + (D^{-1}A) \otimes I_n.$$

The block diagonal matrix  $I_m \otimes T$  is diagonalized by a fast Fourier transform with known eigenvalues. This leaves  $m$  uncoupled tridiagonal systems to be solved, which leads to an  $O(mn \log n)$  algorithm. Details can be found in [3]. As we shall see below, the discrete DtN boundary condition is easily incorporated into this algorithm.

### 3. THE DTN BOUNDARY CONDITION

**3.1. The DtN mapping.** We introduce the finite computational domain  $\Omega$  to be the region bounded by the circle  $\mathcal{B}$  of radius  $\rho_1$  about the origin and the curve  $\gamma$ . The radius  $\rho_1$  is chosen large enough for  $\gamma$  to lie completely in the circle's interior. In addition, we assume that the support of the source function  $f$  in (1) is contained in this circle as well. To find an appropriate boundary condition on  $B$ , we solve the exterior problem

$$(8) \quad \mathbf{A}u + k^2u = 0 \quad \text{in ext}(\mathcal{B})$$

$$(9) \quad u = u(\rho_1, \theta) \quad \text{on } \mathcal{B}$$

$$(10) \quad \lim_{r \rightarrow \infty} r^{\frac{d-1}{2}} (u_r - iku) = 0.$$

The solution can be found by separation of variables to be cf. [9]

$$(11) \quad u(r, \theta) = \frac{1}{\pi} \sum_{\nu=0}^{\infty} \frac{H_{\nu}^{(1)}(kr)}{H_{\nu}^{(1)}(k\rho_1)} \int_0^{2\pi} u(r, \theta') \cos \nu(\theta - \theta') de'$$

where  $H_{\nu}^{(1)}$  is the Hankel function of the first kind of order  $\nu$  and the primed summation symbol indicates that the first term in the series is multiplied by  $\frac{1}{2}$ . Since the series converges uniformly, we can differentiate it with respect to  $r$  term by term. Evaluating this for  $r = \rho_1$  gives

$$(12) \quad u_r(\rho_1, \theta) = \frac{k}{\pi} \sum_{\nu=0}^{\infty} \frac{H_{\nu}^{(1)'}(k\rho_1)}{H_{\nu}^{(1)}(k\rho_1)} \int_0^{2\pi} u(r, \theta') \cos \nu(\theta - \theta') de' =: (Mu)(\rho_1, \theta).$$

Equation (12) expresses the Neumann data  $u_r(\rho_1, \theta)$  in terms of the Dirichlet data  $u(\rho_1, \theta)$  on  $B$ , hence the mapping  $M$  is called the *Dirichlet to Neumann map*. It provides the proper boundary condition on  $\mathcal{B}$ . The continuous problem on the computational domain thus becomes

$$(13) \quad -\mathbf{A}u - k^2u = f \quad \text{in } \Omega$$

$$(14) \quad u = g \quad \text{on } \mathbf{Y}$$

$$(15) \quad u_r = Mu \quad \text{on } \mathcal{B}.$$

**3.2. The discrete radiation condition.** For the rest of this section, we assume that the inner boundary curve  $y$  is a circle about the origin with radius  $\rho_0 < \rho_1$  so that the computational domain is the **annulus**  $\Omega = \mathcal{A}(\rho_0, \rho_1)$ . Once we have determined how to discretize the **DtN** boundary condition, we can incorporate it into the fast solvers for the **annulus** described in section 2 and solve the problem,

$$(16) \quad -\Delta u - k^2 u = f \quad \text{in } \Omega$$

$$(17) \quad u(\rho_0, \theta) = g(\theta)$$

$$(18) \quad u_{,\nu} = M u \quad \text{on } \mathcal{B}.$$

The resulting fast solvers for (16)-(18) will then be combined with an inbedding technique in section 4 to **accomodate** more irregular boundary curves  $y$ .

To discretize (12), the integral is approximated with the trapezoidal rule, which has the same order of accuracy as the finite difference method defined by (5). If we also truncate the infinite series after the first  $N + 1$  terms, the discretized **DtN** boundary condition becomes

$$\begin{aligned} \frac{u_{m+1,p} - u_{m-1,p}}{2\Delta r} &= \frac{k}{\pi} \sum_{\nu=0}^N \frac{H_{\nu}^{(1)\prime}(k\rho_1)}{H_{\nu}^{(1)}(k\rho_1)} \sum_{q=1}^n u_{m,q} \cos\left(\nu(p-q)\frac{2\pi}{n}\Delta\theta\right) \\ &=: C[u_{m,1} u_{m,2} \dots u_{m,n}]^T, \end{aligned}$$

where  $p = 1, \dots, n$  and the matrix  $C$  is given by the sum of matrices

$$C = \sum_{\nu=0}^N e_{\nu} C_{\nu}$$

with coefficients

$$e_{\nu} = \frac{k H_{\nu}^{(1)\prime}(k\rho_1)}{\pi H_{\nu}^{(1)}(k\rho_1)} \Delta\theta$$

and matrices  $C_{\nu}$  given by

$$(C_{\nu})_{pq} = \cos \nu(q-p)\frac{2\pi}{n} =: c_{(q-p)\bmod n}.$$

Thus, each of the matrices  $C_{\nu}$  is circulant. We also note here that the matrix  $C$  is symmetric but not Hermitian, due to the complex values of the Hankel functions. Matrices with this property are known as ‘complex-symmetric’ matrices.

The question of how many terms to retain in the series is answered in [9] by choosing  $N$  such that the error incurred by the truncation of the series is on the same order as the error of the discretization method being used. They give the heuristic formula

$$(19) \quad N_{\text{optimal}} = -p \frac{\log h}{\log \rho_1}$$

where  $p$  is the order of the discretization error and  $h$  is a measure of the mesh spacing.

The matrices  $C_{\nu}$ ,  $\nu = 0, \dots, N$  are all circulant matrices with discrete cosines as entries. We now show that the matrix  $C$  describing the discrete **DtN** boundary condition has only very few distinct eigenvalues.

**Proposition 3.1.** *The non-zero eigenvalues  $\lambda_j^{(\nu)}$   $j = 0, 1, \dots, n-1$  of the matrices  $C_\nu$ ,  $\nu = 0, \dots, N$  are given by*

$$\lambda_\nu^{(\nu)} = \begin{cases} \frac{n}{2} & \text{for } \nu = 0, \frac{n}{2} \\ n & \text{for } \nu \neq 0, \frac{n}{2} \end{cases}$$

and

$$\lambda_{n-\nu}^{(\nu)} = \frac{n}{2}.$$

*Proof.* An arbitrary circulant matrix

$$C = \begin{bmatrix} c_0 & c_1 & \cdots & c_{n-1} \\ c_{n-1} & c_0 & \cdots & c_{n-2} \\ \vdots & \vdots & \ddots & \vdots \\ c_1 & c_2 & \cdots & c_0 \end{bmatrix}$$

has the orthogonal system of eigenvectors  $\mathbf{z}_j$ ,  $j = 0, \dots, n-1$  given by

$$(\mathbf{z}_j)_s = e^{i\frac{2\pi}{n}js}.$$

The corresponding eigenvalues are given by

$$\zeta_j = \sum_{s=0}^{n-1} c_s e^{i\frac{2\pi}{n}js}, \quad j = 0, \dots, n-1.$$

Inserting the entries of  $C_\nu$  determines the eigenvalues  $\lambda_j^{(\nu)}$  to be

$$\lambda_j^{(\nu)} = \sum_{s=0}^{n-1} c_s^{(\nu)} e^{i\frac{2\pi}{n}js} = \sum_{s=0}^{n-1} \cos \frac{2\pi}{n}js \left[ \cos \frac{2\pi}{n}js + i \sin \frac{2\pi}{n}js \right].$$

Applying the orthogonality relations among discrete sines and cosines yields the desired result.  $\square$

Since they all have a common system of linearly independent eigenvectors, the eigenvalues of  $C$  can be determined by summing those of the  $C_\nu$  with the same index. Under the additional assumption that the number of terms in the discrete DtN boundary condition is chosen so that  $N < n/2$ , we have  $0 \leq \nu < n/2$  for all  $\nu = 0, \dots, N$  and the  $N+1$  distinct non-zero eigenvalues of  $C$  are

$$\begin{aligned} \lambda_0 &= ne_0 \\ \lambda_1 &= \lambda_{n-1} = \frac{n}{2}e_1 \end{aligned}$$

$$\lambda_N = \lambda_{n-N} = \frac{n}{2}e_N.$$

The assumption concerning  $N$  is not restrictive, as the optimal values for  $N$  suggested by (19) are much less than  $n/2$ .

**3.3. Combination with fast solvers.** The discrete formulation of (16)-(18) in the first ordering described in section 2 is given by

$$(20) \quad B_{cr} - 2\Delta r b_m S \tilde{C} \mathbf{u} = S \mathbf{f},$$

with  $\mathbf{u}$ ,  $S$  and  $\mathbf{f}$  as in (6) and (7) with  $h \equiv 0$ . The matrix  $\tilde{C}$  is given by

$$(\tilde{C})_{pq} = \begin{cases} (C)_{\frac{p}{n}, \frac{q}{n}} & \text{if } p, q \equiv 0 \pmod{n} \\ 0 & \text{otherwise.} \end{cases}$$

Thus, in the linear system (21), the coefficient matrix is  $B_{cr}$  perturbed by a matrix having  $N + 1$  distinct non-zero eigenvalues. This fact makes preconditioned Krylov subspace methods for non-Hermitian systems attractive for the solution of (21). If  $B_{cr}$  is chosen as the preconditioner, QMR or GMRES will for instance converge in at most  $N + 1$  iterations (cf. [6]). Since the preconditioning can be accomplished using the fast solver introduced in section 2, this results in an efficient solution method.

The discrete DtN condition fits even better into the Fourier technique. Using the second ordering from section 2, the linear system is

$$(21) \quad B_{DtN} \mathbf{u} := B_F - \frac{2\Delta r b_m}{d_m} \begin{bmatrix} 0 & & & \\ & \ddots & & \\ & & \mathbf{1} & \\ & & 0 & c \end{bmatrix} \mathbf{u} = S \mathbf{f}.$$

Here,  $\mathbf{u}$ ,  $\mathbf{f}$  and the scaling matrix  $S$  are assumed permuted conforming with the ordering along circular gridlines described in section 2.2. Setting

$$\alpha_i := \frac{a_i}{d_i}, \quad \beta_i := \frac{a_i + b_i - k^2}{d_i} \quad \text{and} \quad \gamma_i := \frac{b_i}{d_i},$$

the coefficient matrix is

$$\begin{bmatrix} T + \beta_1 I & -\gamma_1 I & & \\ -\alpha_2 I & T + \beta_2 I & -\gamma_2 I & \\ & & \ddots & \\ & & & -\alpha_{m-1} I & T + \beta_{m-1} I & -\gamma_{m-1} I \\ & & & & -(\alpha_m + \gamma_m) I & T - 2\Delta r \gamma_m C + \beta_m I \end{bmatrix}.$$

The matrices  $T$  and  $C$  are both circulant and thus diagonalized by the unitary matrix

$$V = \frac{1}{\sqrt{n}} \left\{ e^{\frac{2\pi i}{n} pq} \right\}_{p,q=0}^{n-1},$$

the multiplication of which by a vector can be accomplished by the fast Fourier transform in  $O(n \log n)$  operations. The eigenvalues of  $T$  are given by

$$\tau_j = 4 \sin^2 \frac{j\pi}{n} \quad j = 0, \dots, n-1$$

and those of  $C$  by

$$\lambda_j = \begin{cases} ne_0 & j = 0 \\ \frac{n}{2}(e_j + e_{n-j}) & j = 1, \dots, n-1 \end{cases}$$

if we assume that no more than  $n$  terms are retained in the discrete DtN boundary condition. If the coefficient matrix is transformed, i.e. multiplied from the left by  $I_m \otimes V$  and from the right by  $I_m \otimes V^H$ , it becomes

$$\hat{B}_{DtN} = \left[ \begin{array}{ccc} D_T & & \\ & \ddots & \\ & & D_T \\ & & & D_T - \frac{2\Delta r b_m}{d_m} D_C \end{array} \right] \left| \begin{array}{c} \dagger \\ (D^{-1}A) \otimes I_n \end{array} \right.$$

where  $D_T = \text{diag}(\tau_j)$  and  $D_C = \text{diag}(\lambda_j)$ . The transformed matrix  $\hat{B}_{DtN}$  is block tridiagonal with diagonal blocks and hence can be decoupled into  $m$  independent tridiagonal linear systems

$$(22) \left| \begin{array}{cccc} \tau_i + \beta_1 & -\gamma_1 & & \\ -\alpha_2 & \tau_i + \beta_2 & -\gamma_2 & \\ & \ddots & \ddots & \ddots \\ & & -\alpha_{m-1} & \tau_i + \mathbf{P}_{m-1} \\ & & & -(\alpha_m + \gamma_m) & \tau_i + 2\Delta r \gamma_m + \mathbf{P}_m \end{array} \right| \left| \begin{array}{c} \hat{\mathbf{u}} = \widehat{\mathbf{S}}\mathbf{f}. \end{array} \right.$$

Here,  $i = 1, \dots, m$  and  $\hat{\mathbf{u}}$  consists of the transformed variables

$$\hat{\mathbf{u}} = \begin{bmatrix} \hat{\mathbf{u}}_1 \\ \vdots \\ \hat{\mathbf{u}}_m \end{bmatrix}, \quad \hat{\mathbf{u}}_i = \begin{bmatrix} \hat{u}_{i,1} \\ \vdots \\ \hat{u}_{i,m} \end{bmatrix},$$

the corresponding indexing being used in the transformed right hand side  $\widehat{\mathbf{S}}\mathbf{f}$ . These systems are solved in  $O(m)$  operations each, after which the solution is obtained by transforming back:

$$\mathbf{u} = (I_m \otimes V^H)\hat{\mathbf{u}}.$$

Thus, the classical Fourier algorithm can be applied to the radiative Helmholtz problem on the annulus  $\mathcal{A}(\rho_0, \rho_1)$ , leading to an overall complexity of  $O(mn \log n)$  operations. If a parallel architecture with  $m$  processing elements is available, this can be reduced to  $O(n \log n)$  by solving the  $m$  independent tridiagonal systems (22) in parallel.

#### 4. IMBEDDING VIA THE CAPACITANCE MATRIX METHOD

**4.1. The imbedding.** The capacitance matrix method is a computational technique for solving the linear systems of equations arising from discretized partial differential equations on irregularly shaped domains. It has been used for solving Poisson and Helmholtz equations, originally in a finite difference framework [4, 10] and more recently also in conjunction with the finite element method cf.[11, 5, 2].

The basic idea is to represent the matrix describing the discretization of the problem on the irregular domain as a low rank modification of the matrix belonging to the discretization of a problem involving the same differential equation on a regularly shaped domain, i.e one whose boundary lies along coordinate lines thus allowing separation of variables. The advantage of this is that fast solvers can be used on the latter problem. The solution of the original problem is then obtained by solving a dense linear system of equations of low dimension  $p$ , the capacitance

matrix equation. The number  $p$  is on the order of the number of gridpoints or finite elements necessary to discretize the irregular boundary. In the original algorithm of [4],  $p$  applications of the fast solver are necessary to generate the capacitance matrix, resulting in an overall complexity of  $O(pN^2 \log N)$  if the original system has the dimension  $N^2$ . Later, it was found by Proskurowski and Widlund [10] that this could be reduced to  $O(N^2 \log N)$  by choosing the regular problem such that the Green's function is translation invariant, e.g. by prescribing periodic boundary conditions in the regular problem. This results in the capacitance matrix being circulant and thus completely determined by only one of its columns.

In our case, we choose  $\rho_0 < \rho_1$  such that the annulus  $\mathcal{A}(\rho_0, \rho_1)$  contains the boundary  $\gamma$  of the scatterer. This is the domain into which the computational domain  $\Omega$  is imbedded. Next, we select two integers  $m$  and  $n$  that define an equispaced grid on  $\mathcal{A}(\rho_0, \rho_1)$ . As in [10], we partition the set of gridpoints

$$G_{m,n} = \{(r_i, \theta_j) : i = 1, \dots, m; j = 1, \dots, n\}$$

into the three sets

$$\begin{aligned} \Omega_h &= \{(r_i, \theta_j) : (r_{i\pm 1}, \theta_{j\pm 1}) \in \Omega\}, \\ (C\Omega)_h &= \{(r_i, \theta_j) : (r_i, \theta_j) \notin \Omega\} \\ \text{and } \partial\Omega_h &= G_{m,n} \setminus (\Omega_h \cup (C\Omega)_h). \end{aligned}$$

The first,  $\Omega_h$ , consists of those gridpoints in  $\Omega$  whose four neighbors in the five-point difference stencil used in (5) lie in  $\Omega$  as well. We shall call these *regular points*. The set  $(C\Omega)_h$  consists of those gridpoints outside of  $\Omega$ . These are introduced into the discrete problem by the imbedding. The capacitance matrix method yields (meaningless) solution values at these points as well. Finally,  $\partial\Omega_h$  contains the gridpoints close enough to the boundary  $\partial\Omega$  for at least one of its four stencil neighbors to lie outside of  $\Omega$ . These we call *irregular points*. As an example, Figure 1 shows a polar grid on an annulus into which an airfoil has been imbedded and the points in  $\partial\Omega_h$  marked with circles.

To obtain a discretization of the problem (16)-(18) on  $\mathcal{A}(\rho_0, \rho_1)$ , we can apply the difference formula (5) at all points in  $\Omega_h \cup (C\Omega)_h$ . For the irregular points, we use the Shortley-Weller formula (see [7]) to approximate the Laplacian. This uses nonsymmetric **two-sided** difference formulas involving those stencil neighbors that still lie in  $\Omega$  and replaces those failing to lie in  $\Omega$  with the intersection of grid lines with the boundary  $\gamma$ . In the latter case, the value given by the Dirichlet condition imposed on the boundary  $\gamma$  supplies the values to be used in these difference formulas. This provides a discretization of the Dirichlet condition on the irregularly shaped boundary  $\gamma$ . In addition, it causes the linear system of equations corresponding to only the points in  $\Omega_h \cup \partial\Omega_h$  to be independent of the values at the remaining gridpoints in  $(C\Omega)_h$ . Indeed, if we denote the matrix resulting from the discretization just described by  $A$ , then there exists a permutation  $P$  of the unknowns  $u_{ij}$  such that  $A$  has the form

$$PAP^T = \begin{bmatrix} A_{11} & 0 \\ A_{21} & A_{22} \end{bmatrix},$$

i.e.  $A$  is reducible. This is necessary so as not to influence the computed solution by the choice of the imbedding problem.

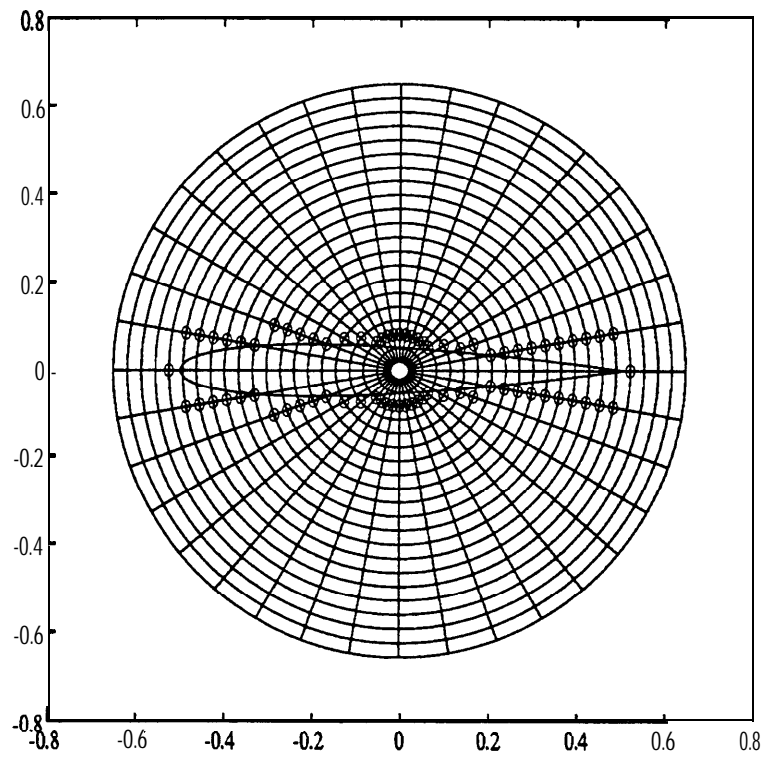


**FIGURE 1.** A NACA0012 airfoil imbedded into a regular polar grid with the points in  $\partial\Omega_h$  marked with 'o'.

On the other hand, if the problem (16)-(18) is discretized without the Dirichlet condition on  $\gamma$ , the resulting matrix is another matrix  $B$ , e.g. the matrix  $B_{Dir}$  in (21) given the proper ordering of the unknowns. The two discretizations only differ in their treatment of the irregular gridpoints. For this reason, the matrices  $A$  and  $B$  only differ in the rows corresponding to these points. Thus, if there are  $p$  points in  $(C\Omega)_h$ , the matrix  $A$  is a rank  $p$  modification of  $B$ . This can be written in the form

$$A = B + UV^T$$

with  $nm \times p$  matrices  $U$  and  $V$ . Each of the  $p$  columns of  $U$  corresponds to **one** of the irregular points in  $\partial\Omega_h$  and has a one at the position corresponding to the index of that point within the grid  $G_{m,n}$  and zeros in all other positions. Thus,  $U$  acts as a discrete extension operator  $U : \partial\Omega_h \rightarrow G_{m,n}$  mapping grid functions defined only on  $\partial\Omega_h$  to grid functions defined on the whole grid and having the value zero for points in  $G_{m,n} \setminus \partial\Omega_h$ . Conversely,  $U^T$  is a discrete trace operator  $U^T : G_{m,n} \rightarrow \partial\Omega_h$  mapping grid functions defined on  $G_{m,n}$  to their restriction to  $\partial\Omega_h$ . The matrix  $V$  is then uniquely determined by

$$V^T = U^T(A - B)$$

since  $U^T U = I_p$ , the  $p \times p$  identity matrix. It can be thought of as a compact representation of the difference  $A - B$ .

Once the matrix  $A$  has been identified as a low rank modification of the matrix  $B$ , linear systems with which can be **efficiently** solved due to the availability of a fast solver, one could use the well-known **Woodbury** formula (cf. [8]), which relates the inverse of  $A$  to that of  $B$ , for solving a linear system with  $A$ . However, as is demonstrated in [10], it turns out that this is numerically unstable for the Dirichlet problem. A stable algorithm is obtained there guided by the integral equations of potential theory.

**4.2. An excursus into potential theory.** In classical potential theory, the solution of Poisson's equation has a representation as the sum of a 'free-space potential' and the potential resulting from a single- or double-layer distribution on the boundary of the region on which the problem is to be solved. For definiteness, take the problem

$$(23) \quad -\Delta u = f \quad \text{in } \Omega$$

$$(24) \quad u_n = g \quad \text{on } \partial\Omega$$

when  $\Omega$  is a bounded domain in  $\mathbb{R}^2$  with smooth boundary. The free-space term in two dimensions is given by

$$u_F(x, y) = \frac{1}{2\pi} \int_{\Omega} f(\xi, \eta) \log \frac{1}{r} d\xi d\eta$$

where  $r = \sqrt{(x - \xi)^2 + (y - \eta)^2}$ . We define the single-layer potential by

$$(25) \quad V(x, y) = \frac{1}{\pi} \int_{\partial\Omega} \rho(\xi, \eta) \log \frac{1}{r} ds(\xi, \eta)$$

and the double layer potential by

$$(26) \quad W(x, y) = \frac{1}{\pi} \int_{\partial\Omega} \mu(\xi, \eta) \frac{\partial}{\partial n(\xi, \eta)} \log \frac{1}{r} ds(\xi, \eta)$$

with smooth functions  $\rho$  and  $\mu$  defined on the boundary  $\partial\Omega$ . The normal derivative is taken with respect to the *inward* normal on the boundary. Using Green's theorem and residual calculations, it is shown that  $V$  and  $\partial W/\partial n$  are continuous across  $\partial\Omega$  while  $\partial V/\partial n$  and  $W$  satisfy jump conditions. In particular, denoting by  $V^+$  the limit of  $V$  approaching  $\partial\Omega$  from the exterior and  $V^-$  from the interior and correspondingly for  $W$ , we have

$$\begin{aligned} V^+ &= V^- \\ \frac{\partial V^\mp}{\partial n} &= \mp \rho + \frac{1}{\pi} \int_{\partial\Omega} \rho \frac{\partial}{\partial n(x, y)} \log \frac{1}{r} ds \\ \frac{\partial W^+}{\partial n} &= \frac{\partial W^-}{\partial n} \\ W^\mp &= \pm \mu + \frac{1}{\pi} \int_{\partial\Omega} \mu \frac{\partial}{\partial n(\xi, \eta)} \log \frac{1}{r} ds. \end{aligned}$$

Inside and outside of  $\Omega$ , the potentials  $V$  and  $W$  are harmonic functions. For the interior Neumann problem above, the successful Ansatz turns out to be

$$u(x, y) = u_F(x, y) + V(x, y).$$

An equation for the yet unspecified function  $\rho$  is obtained by applying the boundary condition, i.e.

$$(27) \quad u_n|_{\partial\Omega} = \frac{\partial u_F}{\partial n} \Big|_{\partial\Omega} + \frac{\partial V^-}{\partial n} = g$$

which, using the jump condition above, yields

$$(28) \quad -\rho + \frac{1}{\pi} \int_{\partial\Omega} \rho \frac{\partial}{\partial n(x, y)} \log \frac{1}{r} ds = \tilde{g}$$

with

$$\tilde{g} = g - \frac{\partial u_F}{\partial n} \Big|_{\partial\Omega}.$$

This is a Fredholm integral equation of the second kind, which constitutes a well-posed problem. It has the form  $(I - K)\rho = \tilde{g}$  with a compact operator  $K$ .

If the same Ansatz is used for the interior Dirichlet problem, proceeding in the same manner results in a first-kind Fredholm integral equation, an ill-posed problem. This is why another Ansatz is necessary, the proper one being

$$u(x, y) = u_F(x, y) + W(x, y).$$

This leads to the equation

$$(29) \quad \mu + \frac{1}{\pi} \int_{\partial\Omega} \mu \frac{\partial}{\partial n(\xi, \eta)} \log \frac{1}{r} ds = \tilde{g}$$

for the function  $\boldsymbol{\mu}$ , where in this case  $\tilde{g} := g - u_F|_{\partial\Omega}$ . In operator notation, this is

$$(I + K^T)\boldsymbol{\mu} = \tilde{g}$$

in which  $K^T$  is the **adjoint** of the operator  $K$ .

The same procedure can be applied to the exterior Neumann and Dirichlet problems, yielding

$$(I + K)\boldsymbol{\rho} = \tilde{g} \text{ and } (I - K^T)\boldsymbol{\mu} = \tilde{g}.$$

It is a discrete analog of the equations (28) and (29) that Proskurowski and Widlund used to derive capacitance matrix equations for the Helmholtz equation

$$-\Delta u + cu = f$$

with non-negative constant  $c$ . For lack of a better idea, this is the approach we have taken to construct our capacitance matrix equations in the case of the radiative Helmholtz equation, where the constant  $c$  is negative.

**4.3. The capacitance matrix method.** Following the continuous case, we make the following Ansatz for the Dirichlet problem:

$$(30) \quad u = B^{-1}\mathbf{f} + 2B^{-1}N\boldsymbol{\mu}.$$

The matrix  $B$  is the matrix of the discrete Helmholtz problem with DtN boundary condition on an **annulus**, into which the scatterer is imbedded. Thus, its inverse  $B^{-1}$  serves as a discrete analog of the free space Green's function and  $B^{-1}\mathbf{f}$  as the discrete free-space potential. The matrix  $N$  is  $nm \times p$  and represents  $p$  discrete dipoles. This is to say that, for a grid function  $v$ , the product  $N^T v \in \mathbb{C}^p$  is an approximation of a constant times the normal derivative of the function  $v$ , which  $v$  approximates, at the irregular mesh points. The constants are chosen such that  $N^T U = I_p$ , which can be achieved by using only exterior points in the approximation formulas of the normal derivative at an irregular point in addition to that point itself. Note also that, with this construction of  $N$ , the vector  $N\xi$ ,  $\xi \in \mathbb{R}^p$  is a grid function vanishing at all interior mesh points, i.e. on all of  $\Omega_h$ . The vector  $\boldsymbol{\mu}$  has  $p$  components and is the analogue of the dipole distribution  $\boldsymbol{\mu}$  in the continuous case. An equation for  $\boldsymbol{\mu}$  is obtained by computing the residual

$$(31) \quad \begin{aligned} Au - f &= (B + UV^T)(B^{-1}\mathbf{f} + 2B^{-1}N\boldsymbol{\mu}) \\ &= (2N + 2UV^TB^{-1}N)\boldsymbol{\mu} + UV^TB^{-1}\mathbf{f}, \end{aligned}$$

From the construction of  $U$  and  $N$ , it follows that the residual vanishes at all points in  $\Omega_h$  independently of  $\boldsymbol{\mu}$ . For it to vanish also on  $\partial\Omega_h$ , we must have, multiplying equation (31) with  $U^T$  and making use of  $U^T U = U^T N = I_p$ :

$$(32) \quad (2I_p + 2V^TB^{-1}N)\boldsymbol{\mu} = -V^TB^{-1}\mathbf{f}.$$

The matrix  $C := (2I_p + 2V^TB^{-1}N)$  is called the *capacitance* matrix and (32) is the *capacitance matrix equation*. The algorithm for solving the original problem can now be summarized as follows:

- (1) Compute  $B^{-1}\mathbf{f}$ .
- (2) Generate the capacitance matrix  $C$  and use  $B^{-1}\mathbf{f}$  to compute the right hand side of (32).

- (3) Solve the capacitance matrix equation.
- (4) Compute  $u$  from (30).

Step (1) can be carried out using the fast solver, after which step (2) requires  $p$  applications of the fast solver, since the matrix  $N$  has  $p$  columns. If one neglects the effort needed to solve the (dense)  $p \times p$  capacitance matrix equation, this produces a complexity of  $O(pnm \log n)$  operations to solve the imbedding problem. Neglecting the effort for solving the capacitance matrix equation is justified by the results of [12], where it is shown that Krylov subspace methods, in that particular case CG applied to the normal equations, can solve this problem very efficiently. This is a direct consequence of using discrete analogues of the integral equations (28) and (29). In future work, we intend to look at more modern methods for non-symmetric systems such as GMRES or QMR for solving the capacitance matrix equation.

In [10], step (2), in which the capacitance matrix is generated, is performed in only one application of the fast solver by using a translation invariant free space Green's function. This results in the capacitance matrix being circulant and hence determined by just one of its columns, any of which can be obtained with one fast solve. Carrying this idea over to the present problem is another subject for future research.

## 5. NUMERICAL RESULTS

In the first experiment, we solve the exterior problem for  $k = 1$  on a disk centered at the origin with radius  $a = 0.5$ . We place the artificial boundary at  $\rho_1 = 1$  and impose Dirichlet boundary conditions  $u(a, \theta) = \cos(j\theta)$  for various values of  $j$ . Since the internal boundary of the computational domain falls on a grid line, no imbedding is necessary and the whole problem can be solved in one application of the fast solver. Figure 2 shows the grid in the case  $m = n = 10$ .

Table 1 shows the maximum deviation  $\|e^{(j)}\|$  of the computed solution to the exact solution

$$u(r, \theta) = \cos j\theta \frac{H_j^{(1)}(kr)}{H_j^{(1)}(k\rho_1)}$$

at the gridpoints. The number of terms in the DtN series was chosen as  $N = j$ , as the boundary function is orthogonal to all higher modes. To verify the complexity of the fast solver, the following execution times were clocked using the Beta3 version of MATLAB4 on a SUN SPARCstation4, the environment in which all the computations were done. When the execution time is divided by  $nm \log n$ , the result remains very close to constant as it should. This can be seen in Table 2.

In the second experiment, we solve the previous problem by imbedding the disk  $r = 0.5$  into the annulus  $\mathcal{A}(0.3, 1)$  with. This is the simplest possible case for the imbedding method, as the boundary of the domain to be imbedded is a coordinate line. The grid spacing is chosen so that the mesh width in the region of the grid exterior to  $r = 0.5$  coincides with that in the previous example. These results are contained in Table 3, a picture of the grid with the irregular points marked is shown in Figure 3.

This exact agreement with the discretization is removed in the next test case, where the scatterer is again a disk, but now is no longer centered at the origin cf.

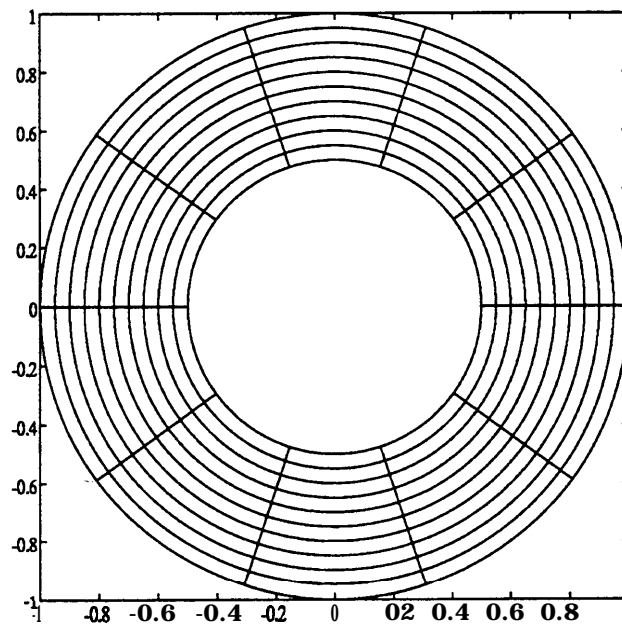


FIGURE 2. The grid used in the first example, no imbedding

m	n	$\ e^{(0)}\ _\infty$	$\ e^{(3)}\ _\infty$	$\ e^{(5)}\ _\infty$
10	10	2.6466(-4)	5.7616(-2)	1.5923(-1)
20	20	6.6217(-5)	1.4424(-2)	4.0189(-2)
30	30	2.9434(-5)	6.4079(-3)	1.7743(-2)
40	40	1.6558(-5)	3.6047(-3)	9.9555(-3)
50	50	1.0597(-5)	2.3074(-3)	6.3627(-3)
60	60	7.3593(-6)	1.6024(-3)	4.4145(-3)
70	70	5.4069(-6)	1.1772(-3)	3.2421(-3)
80	80	4.1396(-6)	9.0129(-4)	2.4822(-3)
90	90	3.2708(-6)	7.1211(-4)	1.9610(-3)
100	100	2.6494(-6)	5.7681(-4)	1.5881(-3)

TABLE 1. Error of computed solution around disk centered at the origin, no imbedding

m = n	execution time [s]	execution time / $nm \log n$
16	1.19	0.0017
32	4.01	0.0011
64	15.7	0.009
128	66.1	0.008
256	315	0.009
512	1620	0.001

**TABLE 2.** Actual and normalized execution times in seconds for one application of the fast solver to solve problem 2

$m$	$n$	$\ e^{(0)}\ _{\infty}$	$\ e^{(3)}\ _{\infty}$	$\ e^{(5)}\ _{\infty}$
10	10	2.6466(-4)	5.7616(-2)	1.5923(-1)
20	20	6.6217(-5)	1.4424(-3)	4.0187(-2)
30	30	2.9434(-5)	6.4079(-3)	1.7743(-2)
40	40	1.6557(-5)	3.6047(-3)	9.9555(-3)
50	50	1.0597(-5)	2.3074(-3)	6.3627(-3)
60	60	7.3593(-6)	1.6024(-3)	4.4144(-3)
70	70	5.4069(-6)	1.7724(-3)	2.4823(-3)
80	80	4.1396(-6)	9.0129(-4)	2.4822(-3)
90	90	3.2708(-6)	7.1211(-4)	1.9610(-3)
100	100	2.6494(-6)	5.7681(-4)	1.5881(-3)

**TABLE 3.** Error of computed solution around disk centered at the origin with imbedding

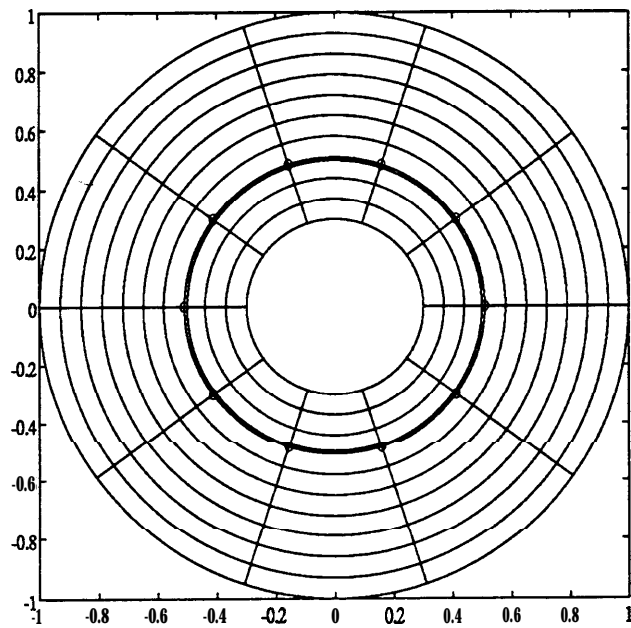


**FIGURE 3.** Grid used in the second problem, centerde circle imbedded into an annulus

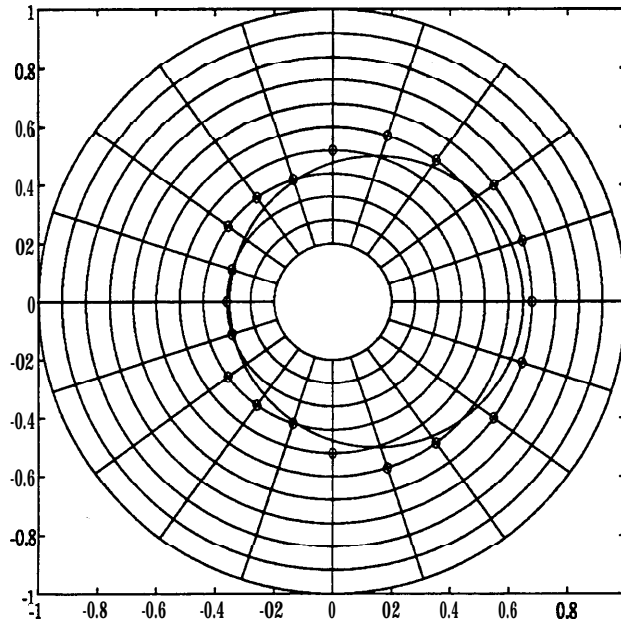


**FIGURE 4.** The grid used in the third problem, non-centered disk imbedded into an annulus

Figure 4). In all the test cases, the exact solution is given by 11, where the series consists of only one term due to the choice of the Dirichlet boundary condition.

Finally, we attempt a more application oriented problem where the scattering body is a NACA0012 airfoil. We display the solution time needed to solve the whole problem for various mesh widths. Figure 1 shows the grid and the airfoil with the irregular boundary points marked.

#### REFERENCES

1. A. Bayliss, M. Gunzburger, and E. Turkel, *Boundary conditions for the numerical solution of elliptic equations in exterior domains*, *SIAM J. Appl. Math.* **42** (1982), 430-451.

$m$	$n$	$\ e^{(0)}\ _{\infty}$	$\ e^{(1)}\ _{\infty}$	$\ e^{(2)}\ _{\infty}$
10	20	8.6345(-4)	2.0732(-2)	2.6998(-2)
20	40	3.0620(-4)	1.1100(-2)	1.6434(-2)
40	80	1.4390(-4)	6.1266(-3)	9.8803(-3)
80	160	1.0299(-4)	3.0513(-3)	8.3530(-3)

**TABLE 4.** Error of the solution to the problem on exterior of non-centered circle using imbedding

$m$	$n$	$p$	execution time [s]	execution time/ $mnp$ log n
20	60	98	159	3.302(-3)
30	90	146	478	2.695(-3)
40	120	194	1093	2.452(-3)
50	150	244	2109	2.300(-3)
60	180	292	3747	2.299(-3)

TABLE 5. Error of the solution to the problem on exterior of non-centered circle using imbedding

2. C. Börgers and O. B. Widlund, *Finite element capacitance matrix methods*, Tech. Report 261, Computer Science Dept., New York University, 251 Mercer Street, New York, N.Y. 10012, 1986.
3. B. Buzbee, G. Golub, and C. Nielson, *On direct methods for solving Poisson's equation*, SIAM J. Numer. Analysis 7 (1970), 627-656.
4. B.L. Buzbee, F.W. Dorr, J.A. George, and G.H. Golub, *The direct solution of the discrete Poisson equation on irregular regions*, SIAM J. Numer. Anal. 8 (1974), 722-736.
5. M. Dryja, *A finite-element capacitance matrix method for the elliptic problem*, SIAM J. Numer. Anal. 20 (1974), 621.
6. O. Ernst and G. Golub, *A domain decomposition approach to solving the Helmholtz equation with a radiating boundary condition*, Tech. Report NA-92-08, Stanford University, Computer Science Dept., August 1992.
7. G.E. Forsythe and W.R. Wasow, *Finite-difference methods for partial differential equations*, Wiley, 1960.
8. A.S. Householder, *The theory of matrices in numerical analysis*, Dover, 1964.
9. J. B. Keller and D. Givoli, *Exact non-reflecting boundary conditions*, J. Comput. Phys. 82 (1989), 172-192.
10. W. Proskurovski and O. B. Widlund, *On the numerical solution of Helmholtz' equation by the capacitance matrix method*, Math. Comp. 30 (1976), 433-468.
11. ———, *A finite element capacitance matrix method for the Neumann problem for Laplace's equation*, SIAM J. Sci. Statist. Comput. 1 (1980), 410.
12. A. Shieh, *On the convergence of the conjugate gradient method for singular capacitance matrix equations from the Neumann problem of the Poisson equation*, Numer. Math. 29 (1978), 307.
13. P. N. Swarztrauber and R. A. Sweet, *The direct solution of the discrete Poisson equation on a disk*, SIAM J. Numer. Analysis 10 (1973), 900907.
14. R. A. Sweet, *A cyclic reduction algorithm for block ttidiagonal systems of arbitrary dimension*, SIAM J. Numer. Analysis 14 (1977), 706-720.

SCIENTIFIC COMPUTING & COMPUTATIONAL MATHEMATICS PROGRAM, STANFORD UNIVERSITY,  
STANFORD, CA 94305

E-mail address: ernst@sccm.stanford.edu